

引用格式:周璇,李乔磊,张婷婷,等.光固化增材制造陶瓷型芯缺陷分析及调控机制研究进展[J].材料工程,2026,54(2):15-27.
ZHOU Xuan, LI Qiaolei, ZHANG Tingting, et al. Research progress in defect analysis and regulation mechanism of ceramic cores in stereolithographic additive manufacturing[J]. Journal of Materials Engineering, 2026, 54(2): 15-27.

光固化增材制造陶瓷型芯缺陷分析及调控机制研究进展

周 璇^{1,2}, 李乔磊^{2*}, 张婷婷², 岳新艳¹, 梁静静^{2,3}, 李金国^{2,3}

(1 东北大学 材料科学与工程学院, 沈阳 110819; 2 中国科学院金属研究所 师昌绪先进材料创新中心, 沈阳 110016; 3 中国科学院太空制造技术重点实验室, 北京 100094)

摘要:高温合金空心涡轮叶片是航空发动机的核心高温部件,而用于叶片内部复杂的冷却流道结构成型的陶瓷型芯是叶片制备的关键过渡部件。光固化增材制造陶瓷型芯工艺具有无需模具、精度高、工艺周期短等优点,为复杂结构陶瓷型芯的高精度制备提供了一种可靠的新工艺,其中型芯增材制造过程中的缺陷控制成为高精度陶瓷型芯制备的关键。本文概述了国内外对打印缺陷、脱脂-烧结缺陷控制的研究进展,归纳了缺陷调控机制,从浆料制备、打印成型、脱脂-烧结工艺优化和矿化剂添加等方面综述了缺陷调控的研究现状。在此基础上,提出固化行为、孔隙分布规律与深度学习是未来研究陶瓷型芯的重要发展方向。

关键词:增材制造;陶瓷型芯;缺陷;涡轮叶片;精密铸造

doi: 10.11868/j.issn.1001-4381.2025.000376 **CSTR:** 32421.14.j.issn.1001-4381.2025.000376

中图分类号: TB32; TQ174.75 **文献标识码:** A **文章编号:** 1001-4381(2026)02-0015-13

Research progress in defect analysis and regulation mechanism of ceramic cores in stereolithographic additive manufacturing

ZHOU Xuan^{1,2}, LI Qiaolei^{2*}, ZHANG Tingting², YUE Xinyan¹, LIANG Jingjing^{2,3}, LI Jinguo^{2,3}

(1 School of Materials Science and Engineering, Northeastern University, Shenyang 110819, China;
2 Shi-changxu Innovation Center for Advanced Materials, Institute of Metal Research, Chinese Academy of Sciences, Shenyang 110016, China; 3 CAS Key Laboratory of Space Manufacturing Technology, Beijing 100094, China)

Abstract: Superalloy hollow turbine blades are key components of aero engines, and the ceramic core used for forming the complex cooling channel structure inside the blade is a key transitional component in the blade preparation. The stereolithographic additive manufacturing process for ceramic cores has the advantages of no need for molds, high precision, and short process cycle, providing a reliable new process for the high-precision preparation of complex-structured ceramic cores. Among them, defect control in the additive manufacturing process of cores has become the key to the preparation of high-precision ceramic cores. This work summarizes the current research status of printing, degreasing and sintering defect control at home and abroad. The defect regulation mechanism is summarized, and the research status of defect regulation is reviewed from aspects such as slurry preparation, printing and degreasing-sintering process optimization, and the addition of mineralizers. On this basis, it is proposed that curing behavior, pore distribution law and deep learning are important development directions for future research on ceramic cores.

Key words: additive manufacturing; ceramic core; defect; turbine blade; precision casting

高温合金空心涡轮叶片作为航空发动机的核心高温部件,其性能水平(特别是承温能力)是衡量发动

机先进程度的重要标志,并且在一定程度上反映了国家的工业制造水平^[1-2]。为了提高航空发动机的推重

比,对空心涡轮叶片的承温能力提出了更高的要求,相关技术成为研究学者关注的焦点。提高涡轮叶片承温能力的措施主要包括开发更高承温能力的高温合金新材料、优化热障涂层构筑和叶片冷却结构等。优化叶片冷却结构、提高叶片冷却效率是目前提高涡轮叶片承温能力最有效的措施,而陶瓷型芯的制造技术则是实现这一目标的核心^[3-5]。

陶瓷型芯的传统成型工艺主要有热压注成型、传递成型、灌浆成型,其中热压注陶瓷型芯制备工艺利用模具进行成型,成型后的陶瓷型芯质量稳定,在简单结构陶瓷型芯的批产中被广泛应用^[6]。由于涡轮叶片内部冷却流道越来越复杂,型芯的传统制造工艺在制备复杂结构型芯时面临巨大的挑战,这极大地制约了涡轮叶片冷却流道及其设计技术的发展。光固化增材制造技术为复杂异形陶瓷型芯的成型提供了全新的技术方案,它是利用紫外光使含有陶瓷粉体的光敏树脂发生交联反应,逐层固化叠加,最终转化为三维实体。该技术具有高精度、低成本和设计自由度高等优点,逐渐成为复杂结构陶瓷部件制备最具前景的关键成型技术之一^[7]。但在增材制造过程中打印缺陷与脱脂-烧结缺陷阻碍了该技术在复杂结构陶瓷型芯制备领域更广泛的应用^[8-9]。

本文结合国内外研究进展,梳理了增材制造陶瓷

型芯的打印缺陷与脱脂-烧结缺陷类型,并针对其产生原因,从浆料制备、打印工艺优化、烧结参数优化、矿化剂助烧等角度进行了调控机制的归纳,总结了各种调控手段对增材制造陶瓷型芯的性能影响。在此研究现状的基础上,展望了未来光固化增材制造陶瓷型芯的研究方向和发展趋势。

1 光固化增材制造陶瓷型芯缺陷类型及产生机制

1.1 增材制造陶瓷型芯打印缺陷研究现状

利用光固化3D打印技术制备陶瓷型芯时,首先需要将陶瓷粉末、光敏树脂、光引发剂、分散剂等按比例混合,制备陶瓷浆料,随后在紫外光的照射作用下,光敏树脂发生交联固化,逐层堆叠得到型芯素坯。在这一过程中会出现打印孔隙、打印裂纹、打印错层和打印变形等缺陷,如图1所示^[10-11]。Wang等^[12]发现随着打印孔隙的增多,陶瓷样品的体积密度由 $3.0135\text{ g}\cdot\text{cm}^{-3}$ 降至 $2.8382\text{ g}\cdot\text{cm}^{-3}$ 。Puchakayla等^[13]通过实验验证,经过氧化钇预处理的氧化锆陶瓷中的孔隙体积分数降至11%,从而使烧结后的样品强度上升。过多的打印孔隙在影响陶瓷素坯本身的性能时,也会危害烧结后的样品性能。Li等^[14]指出打印裂纹的产生使铝基

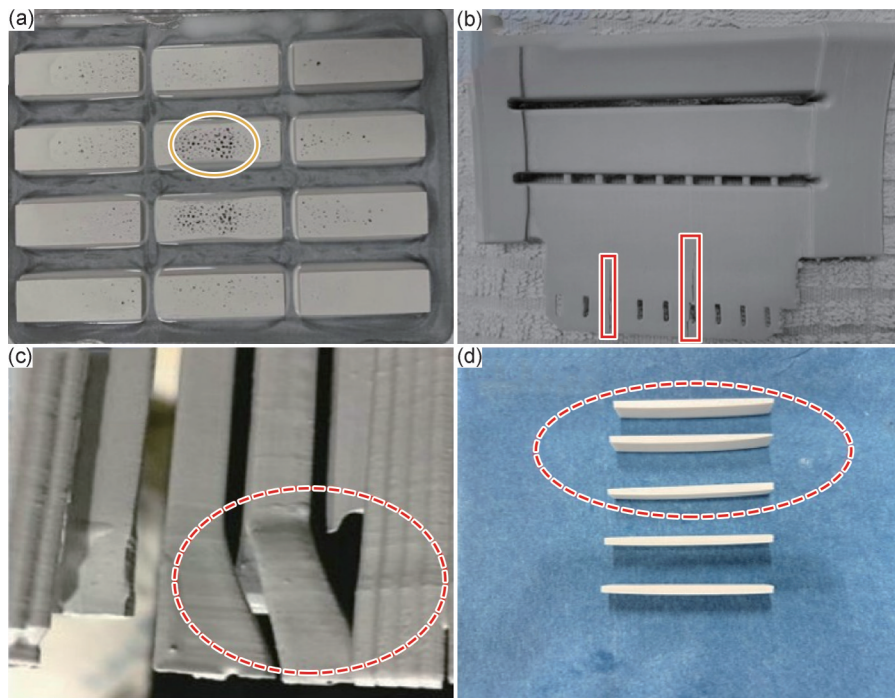


图1 陶瓷型芯的打印缺陷

(a)打印孔隙;(b)打印裂纹^[10];(c)打印错层^[11];(d)打印变形

Fig.1 Printing defects of ceramic cores

(a)printing pores;(b)printing cracks^[10];(c)printing wrong layer^[11];(d)printing deformation

陶瓷型芯的抗弯强度由 26.5 MPa 降至 14.5 MPa。Nie 等^[15]采用化学沉淀涂层处理的方法提高了 Y_2O_3 在 Al_2O_3 基陶瓷浆料中的分散均匀性,并减少打印裂纹的产生,使样品抗弯强度最高达到 (455.37 ± 32.17) MPa。打印裂纹会显著降低陶瓷型芯的强度。Xing 等^[16]研究发现,随着刮刀速度由 1.5 mm/s 增加至 3.5 mm/s,浆料铺展得更加均匀,打印精度提高,打印错层现象减少。Li 等^[17]探究了单层打印厚度对陶瓷型芯蠕变的影响,发现随着打印厚度的增加,相同蠕变时间内平均变形量由 0.2 mm 升至 0.6 mm。Li 等^[18]研究发现,过高的固化深度会导致单体转化率由 5.2% 降低到 2.0%,产生打印变形。打印错层和打印变形会降低成型精度,对高精度陶瓷型芯的制备造成不利影响。

为了探明上述打印缺陷形成的原因,国内外相关研究学者对打印缺陷的产生机制进行了系统的研究。浆料制备是增材制造陶瓷型芯成型的前提,浆料的性能会影响陶瓷型芯缺陷的产生。浆料中陶瓷颗粒分散不均匀会导致打印层固化效果差异,从而导致片层缺陷不同^[19]。而在浆料铺展过程中,由于浆料中间层

的流速比上下表面的流速快,细颗粒更易于在上下表面聚集^[20],从而导致打印层界面由细颗粒组成,孔隙小且致密。片层结构内部由粗颗粒组成,孔隙大且分散,机理图如图 2 所示。由于陶瓷颗粒的不均匀分布,紫外光在透过浆料时传播路径发生改变,产生能量衰减,衰减后较低的曝光能量密度使固化厚度显著降低,打印层间结合强度不足,导致层间裂纹的产生^[21]。而较长的曝光时间会提高陶瓷粉末沉降的概率,产生树脂富集区域的模糊过渡边界,当打印层彼此接触时,会在另一侧上形成清晰的直线边界的层状结构^[22]。此外,在上提拉式打印过程中素坯需克服浆料阻力才能缓慢浸入树脂液面,这个过程中产生的水平分力会引起素坯变形,当新一层开始曝光固化时,由于素坯发生变形,新固化层仍在理论位置成型,导致与前固化层产生层间错位缺陷,这种缺陷最终表现为打印件表面的阶梯状不规则纹路^[11]。Zhang 等^[23]认为当打印过程中的屈服应力不足以克服浆料本身的表面张力与协同的重力作用时,更容易产生打印变形。表 1^[12,17,21,24-25]总结了光固化过程中常见的打印缺陷类型及其形成机制。

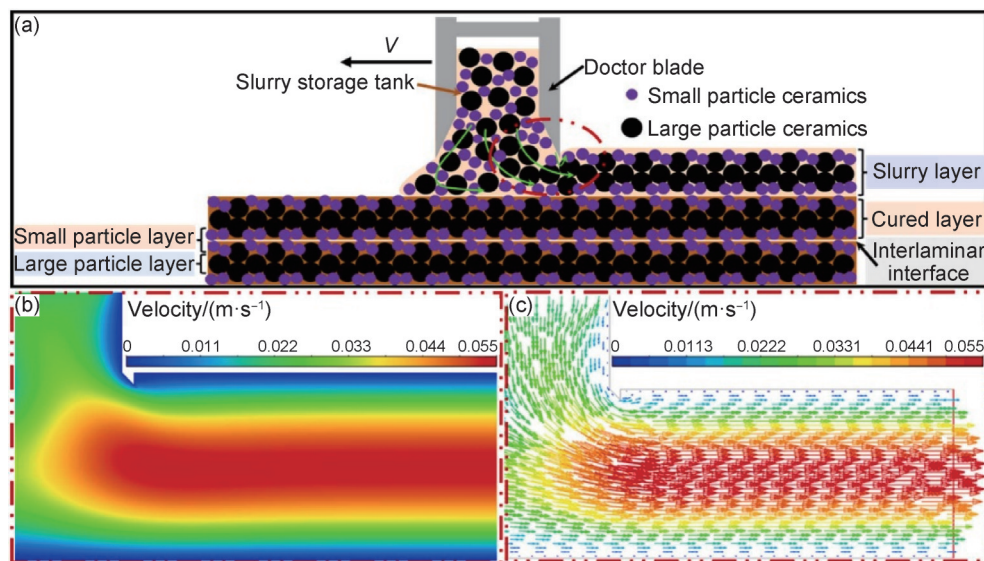


图 2 陶瓷型芯打印层间缺陷产生机理^[20]

Fig.2 Generation mechanism of interlayer defects in ceramic core printing^[20]

综上所述,目前陶瓷型芯在光固化打印过程中产生缺陷的原因主要可以概括为三个方面:(1)紫外光的交互作用:由于紫外光在浆料中的散射和折射,导致某些区域的固化不均匀或出现错误固化区域;(2)打印过程中出现的应力分布不均:在多层打印过程中,当打印层之间的应力分布不均匀时会使得打印层彼此结合不牢而引起层间裂纹;(3)阶梯效应:由于逐层打印的特性,在多层叠加时,样品表面可能出现

阶梯状现象。值得一提的是,固化机制与光传播过程中能量损耗之间的研究目前较少,而这也将成为未来研究的重点方向。

1.2 增材制造陶瓷型芯脱脂-烧结缺陷研究现状

打印成型的陶瓷型芯素坯在经过脱脂-烧结这一过程后才能得到应用。脱脂过程是指将陶瓷型芯素坯在炉内缓慢加热至脱脂温度,并保持适当的时间,使得素坯中的非陶瓷组分脱脂。将脱脂后的素坯持

表1 增材陶瓷型芯打印缺陷类型及形成机制

Table 1 Types and formation mechanisms of printing defects in additive ceramic cores

Defect type	Generation mechanism	Reference
Printing pore	Agglomeration of solid-phase powder during the printing process; when the curing area is insufficient, debonding occurs during the action of the liquid-phase adhesive	[24]
Printing crack	The uneven release of internal stress leads to insufficient interlaminar bonding strength	[17,21]
Printing wrong layer	The reaction resistance of the slurry will cause an error between the actual light-curing area and the theoretical area, resulting in incorrect curing	[12]
Printing deformation	The yield stress during the printing process is insufficient to overcome the surface tension of the slurry itself and the synergistic gravitational effect	[25]

续加热至烧结温度并保温一定时间的过程则被称为烧结过程。在脱脂-烧结过程中会产生脱脂孔洞、脱脂裂纹、烧结孔洞、烧结裂纹等缺陷,如图3所示^[26-29],这些缺陷会对陶瓷型芯的性能产生不利影响。Li等^[30]发现真空脱脂温度处于300~350℃时,氧化铝基陶瓷中的光敏树脂难以完全脱出,从而产生脱脂孔洞。Wang等^[27]同样在低温脱脂环境下验证了脱脂孔洞和脱脂裂纹的存在,并且为了获得最优异的性能,设计了合理的脱脂曲线。Li等^[31]优化出0.5℃/min的脱脂升温速率,使得氧化铝基陶瓷型芯脱脂裂纹减少,抗弯强

度达到27.5 MPa。脱脂孔洞和脱脂裂纹会导致陶瓷型芯的性能下降。Li等^[32]采用MIP技术制备铝基陶瓷型芯,发现当累计孔面积为0.10 m²时,其具有最高的抗弯强度。Liu等^[33]经过实验验证得出烧结孔洞的减少可以提升氧化铝基陶瓷型芯性能的结论,此时制备样品的最大抗弯强度为46.2 MPa。Zhang等^[34]研究发现Al₂O₃在ZrO₂基体陶瓷中的分散可以起到钉扎作用,阻碍烧结裂纹生成。Qiu等^[29]进一步研究证实,减少烧结裂纹可以使陶瓷型芯的抗弯强度显著提升。烧结孔洞和烧结裂纹会降低陶瓷型芯的强度,不利于生产使用。

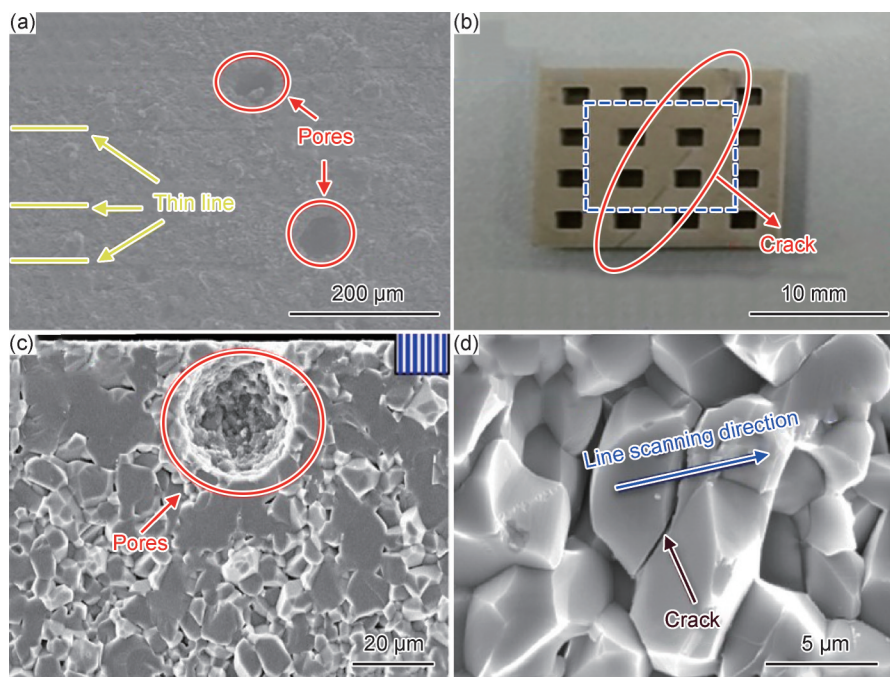


图3 陶瓷型芯的脱脂-烧结缺陷
(a)脱脂孔洞^[26]; (b)脱脂裂纹^[27]; (c)烧结孔洞^[28]; (d)烧结裂纹^[29]

Fig.3 Degreasing-sintering defects of ceramic cores
(a)degreasing holes^[26]; (b)degreasing cracks^[27]; (c)sintering holes^[28]; (d)sintering cracks^[29]

为了解释上述缺陷产生的机制,国内外学者开展了系统的研究。当脱脂温度过低时,气泡夹在素坯里难以逸出,导致脱脂孔洞产生^[35]。在加热过程中,由

于受热部位的不同会导致陶瓷型芯素坯表面的液相率先氧化分解从而形成脆弱的表面层,当温度进一步升高时,这些脆弱的表面层无法抵抗内部的热应力冲

击从而出现裂纹缺陷^[36]。当表面层中的微观空间不足以容纳素坯在高温区热分解时产生的气态分解物及交联聚合物组成的网络状结构时,素坯发生热膨胀;热膨胀和粉体间的毛细管力形成过大压力导致裂纹产生^[37-38]。

烧结过程中,烧结温度会显著影响烧结缺陷的形成。烧结温度过低时,陶瓷颗粒的晶粒生长不充分,再结晶现象占主导地位,但再结晶晶粒的尺寸较小且分布不均匀,烧结颈难以形成^[39]。而当烧结颈异常长

大时,在烧结过程中圆孔被其包覆,气体难以逸出,产生烧结孔洞。由于光固化的整个打印过程是逐层进行的,Li等^[40]研究发现,随着陶瓷颗粒在烧结过程中的再分布,层状结构界面处的孔隙会由均匀分布逐渐向界面孔隙线集中,产生裂纹。烧结温度过高时,陶瓷颗粒之间的结合强度大于陶瓷颗粒自身的结合强度,裂纹穿过陶瓷颗粒扩展,断裂模式由沿晶断裂转变为穿晶断裂。表2^[17,30,41-43]总结概括了增材陶瓷型芯脱脂-烧结时易产生的缺陷类型及形成机制。

表 2 增材陶瓷型芯脱脂-烧结缺陷类型及产生原因

Table 2 Types and causes of defects in the degreasing and sintering of additive ceramic cores

Defect type	Generation mechanism	Reference
Degreasing hole	The binder in the liquid phase is unevenly distributed, and the pressure generated by the discharge of the resin decomposition products hinders its own discharge	[41]
Degreasing crack	The uneven thermal redistribution between the solid-phase inorganic powder system and the liquid-phase organic system generates thermal stress. The pore channels inside the green body become fewer or smaller, hindering the volatilization of the binder	[42]
Sintering hole	When the sintering temperature is too low, the adhesion between particles is poor and it is difficult to form a sintering neck; when the sintering temperature rises, the pores migrate and enrich towards the interlayer interfaces, and the pores merge at the interfaces to form large pores	[17,43]
Sintering crack	The generation of the layered structure causes large pores to aggregate at the interface into pore lines, which become the source of sintering cracks	[30]

综上所述,增材制造陶瓷型芯在脱脂-烧结过程中产生缺陷的主要原因为两个方面:(1)气体排出的速率。当气体排出速率过快时,容易形成气泡,进而产生脱脂孔洞;当气体排出速率过慢时,气体流动不畅通,使得在烧结过程中气体被封闭在颗粒之间,形成烧结孔洞。(2)颗粒之间的应力。当素坯受热不均匀时,颗粒之间的瞬时温度不同会诱发热应力场,此时坯体内部产生显著的应力不匹配;而随着颗粒接触面积由点变成面,这一过程伴随着应力集中,使得陶瓷型芯内部大幅度收缩,产生脱脂裂纹与烧结裂纹,最终导致型芯变形。

2 光固化增材制造陶瓷型芯缺陷调控策略研究

2.1 增材制造陶瓷型芯打印缺陷控制研究现状

在增材制造技术中,理解陶瓷浆料的固化机制是进行陶瓷型芯打印缺陷控制的关键前提。Gentry等^[44]研究发现在光照射陶瓷浆料的过程中,陶瓷浆料的固化宽度和固化深度均随入射光能量的对数呈线性增加,符合准Beer-Lambert关系。

$$D_b = S_d \ln \left(\frac{E_w}{E_d} \right) \quad (1)$$

式中: D_b 为固化深度; S_d 为深度灵敏度,与材料本身的性质有关; E_w 为临界宽度能量; E_d 为临界深度能量。当入射光能量过高时会发生显著的过度增宽,增宽的程度随着能量的增加而增大。由于临界宽度能量显著高于临界深度能量,当入射光能量处于一定的范围时,紫外光照射浆料可以获得一定的固化深度而不会过度加宽。Li等^[45]则在光固化过程中发现了温度的变化,这一现象是由于入射光穿透固化层后发生能量转换而引起的。在 35.6 mJ/cm^2 的入射光能量和 $50 \mu\text{m}$ 的传播长度下,一次固化层达到了最终转化率。在此基础上Gentry解释了光与一次固化层的相互作用,如图4所示(RI代表入射介质的折射率)^[45]。当入射光照射到空气-树脂界面时,一部分发生散射,另一部分穿入固化层内部。由于 $\alpha\text{-Al}_2\text{O}_3$ 的折射率大于树脂的折射率,因此固化层内部发生光散射,导致光传播方向偏离垂直,二次固化能量强度的实际损失值大于理论值。紫外光与各层之间的交互作用不同使得出现错误固化区域的概率上升,从而导致固化深度不足。在打印过程中的应力分布不均匀也会引起层间开裂,而逐层打印的特性会导致阶梯效应的出现。依托固化机制,目前常用的控制陶瓷型芯打印缺陷的手段有构建浆料体系与完善打印工艺。

优化浆料成分和制备工艺,对于提升增材制造陶

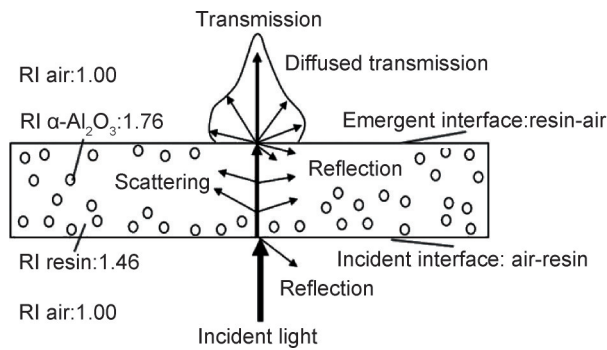


图4 紫外光与浆料层的交互作用机制^[45]

Fig.4 Interaction mechanism between ultraviolet light and the slurry layer.^[45]

瓷型芯的质量至关重要,能显著降低内部缺陷的形成概率。Cai等^[46]将硅基陶瓷浆料的固含量由40%(体积分数,下同)提升至60%时,烧结收缩率由35%降至24%。An等^[47]同样制备了60%的硅基陶瓷浆料,气孔率降至30%。Yang等^[48]通过光固化3D打印技术将硅基陶瓷粉末的固含量从56%提升至68%,随着固含量的增加,堆积密度增加,层间间隙减少,微观结构更均匀。烧结收缩率降低至约3%,层间强度提高至11.43 MPa,同时保持了23.47%的表观孔隙率。Gu等^[49]制备了70%的 Al_2O_3 陶瓷型芯浆料,对比发现其与低固含量的浆料具有相似的固化性能,这是光敏树脂的高固化活性和陶瓷浆料的低散射性共同作用的结果。随着固含量的增加,素坯中的孔洞和翘曲缺陷明显减少,相邻层之间结合力显著增强,浆料的稳定性和打印精度得到提升。

过量的固含量也会带来浆料黏度过大、固化深度和固化宽度较小的问题,目前采用协同调整液相配方的方法来调控。Jin等^[50]发现,HDDA(1,6-己二醇二丙烯酸酯):TMPTA(1,1,1-三甲基丙烷三丙烯酸酯)的比例为6:2时,浆料中总官能团数减少使得浆料黏度降低,紫外光照射树脂时,碳碳双键的打开程度增加,固化性能提高。Chen等^[51]考察了三种常用分散剂对氧化铝陶瓷浆料光固化性能的影响。KOS110配方表现出最低的固化深度,其次是BYK111配方,而BYK180配方表现出最大的横向固化偏差。Fan等^[52]在硅基陶瓷浆料中添加了13%的BYK111+BYK9076分散剂,解决了亲水性陶瓷粉体与油性树脂之间的润湿性差这一问题,降低了浆料黏度。Kim等^[53]研究发现,在PZT陶瓷中BYK142的质量分数为2%时,光能量转化率与光固化速率达到最高。合理的浆料体系可以有效减少增材陶瓷型芯中缺陷的产生。

在光固化增材制造过程中,紫外光在浆料中的散

射和折射会导致诸如台阶效应、孔洞和翘曲等缺陷的产生^[54],而改善打印工艺也是调控增材陶瓷型芯缺陷的有效手段。Mu等^[55]研究了不同固化参数(曝光能量密度和曝光时间)对单层和多层陶瓷芯样品打印质量的影响。当曝光能量过低时,单层固化深度过小,会导致多层样品无法进行层与层之间的分离,从而造成打印失败。随着曝光能量的不断增加,单层固化深度增加,多层试样层间结合强度增大。浆料与先前固化层之间的中间层的再固化行为可以提高结合强度并降低台阶效应。打印方向不同对素坯性能也会有影响,Schlacher等^[28]通过实验发现当沿着打印方向施加载荷时,氧化铝基陶瓷具有固定取向的平面缺陷(例如弱层边界或层间不均匀性),会降低该方向的强度。Basar等^[56]对比了不同打印温度(25、35、45、55℃)对陶瓷浆料流变行为和剥离力的影响。当打印温度接近黏结剂混合物的初始玻璃化转变温度时,浆料的剪切稠化行为得到明显改善,在打印期间浆料得到均匀补充,从而减少层间缺陷。提高打印温度可以增强黏结剂与陶瓷粉末之间的反应活性,从而提高素坯的强度和精度,减少变形和开裂。优化打印工艺可以提升打印质量,减少打印缺陷。

综上所述,现阶段调控打印缺陷的方式主要有增大浆料的固含量,调整浆料液相配方,优化打印工艺。通过综述浆料体系与打印工艺优化的研究现状,改善紫外光的交互作用、消除打印过程中的应力不均、控制浆料中陶瓷颗粒的分布状态是减少增材制造陶瓷型芯缺陷的关键。

2.2 增材制造陶瓷型芯脱脂-烧结缺陷控制研究现状

增材制造陶瓷型芯脱脂-烧结机制如图5所示^[57]。在陶瓷型芯素坯放入炉内脱脂的过程中,坯体内的树脂被去除。伴随着型芯的体积收缩,颗粒与颗粒之间的接触面积增大。当树脂以气体的方式完全逸出后,标志着陶瓷型芯的成型过程进入烧结阶段。在烧结阶段初期,粉末边界受到粉末颗粒之间的接触产生的压应力产生烧结颈。在形成烧结颈后,由于颈部存在弯曲表面,使得颈部凹面的空位浓度高于平均空位浓度,该空位浓度梯度差使原子反向流动到颈部,颈部的周围产生尖锐的菱形孔隙。随着烧结温度不断升高,烧结颈不断长大,烧结体的表面能降低驱使孔隙圆化与致密化。当进入烧结阶段后期时,颗粒的生长成为孔隙进一步致密化的主要原因。总结来看,脱脂-烧结过程中不适的气体排出速率会导致不畅通的排气过程,从而使得孔洞出现。而颗粒之间的应力不均会促使裂纹生成与扩展。依托脱脂-烧结机制,目前常采用改进脱脂-烧结工艺与添加矿化剂的方法来调

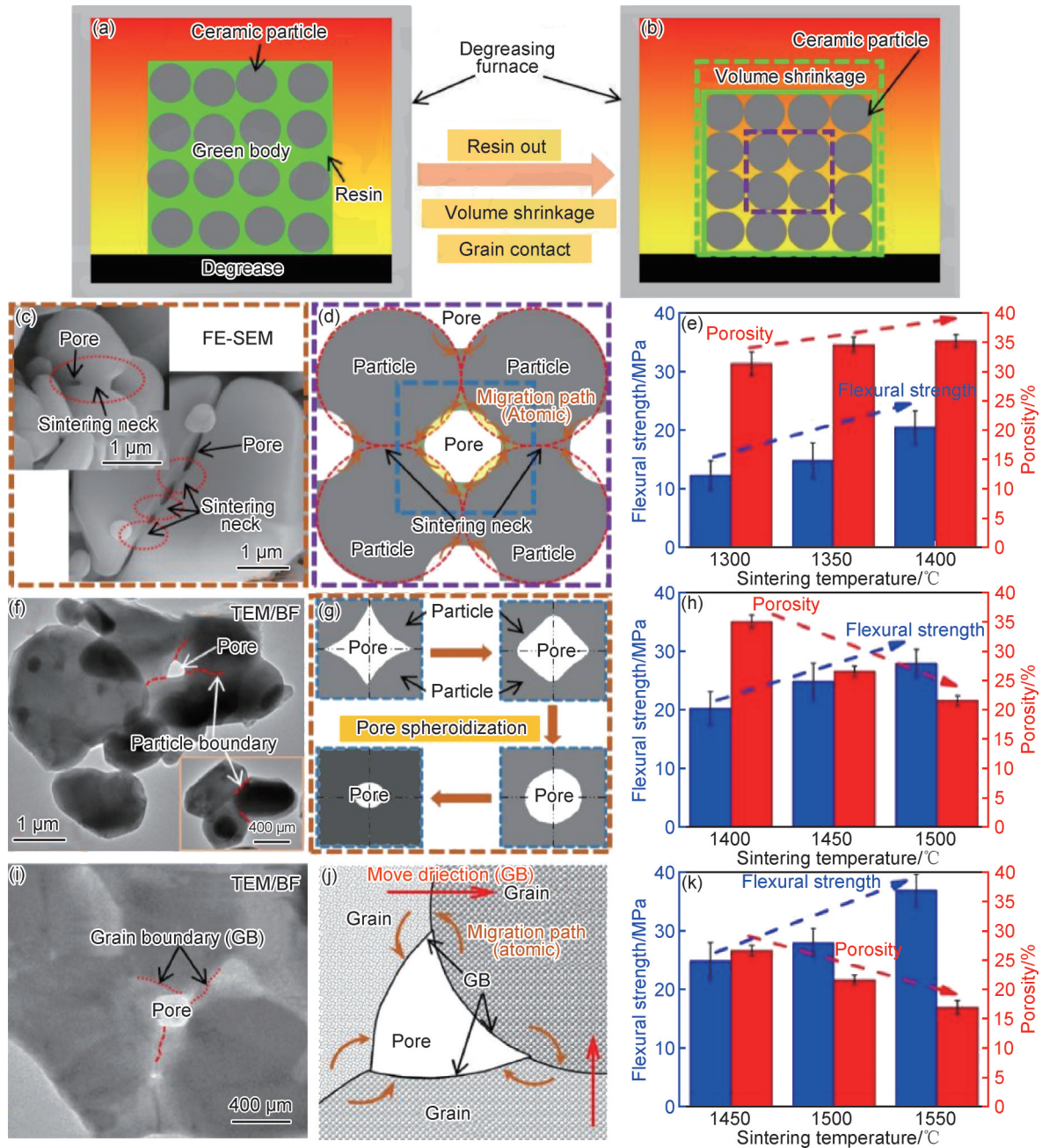


图5 不同烧结阶段对型芯性能影响的机理图^[57]

(a), (b)型芯脱脂和烧结过程; (c)~(e)烧结初始阶段; (f)~(h)烧结中期; (i)~(k)烧结后期

Fig.5 Mechanism diagram of the influence of sintering stage on core performance^[57]

(a), (b)degreasing and sintering process of the core; (c)-(e)initial stage of sintering; (f)-(h)mid sintering stage; (i)-(k)late stage sintering

控陶瓷型芯的脱脂-烧结缺陷。

由于气体的扩散是通过光敏树脂的固化来实现的,脱脂-烧结过程中不同的保温时间与不同的气氛会影响气体的扩散,从而影响陶瓷型芯性能。Li等^[58]发现在真空脱脂 120 min 和氩气脱脂 180 min 后,氧化铝陶瓷型芯的抗弯强度分别达到最大值(26.4±0.7) MPa 和(25.1±0.5) MPa。Li等^[26]研究发现在氩气气氛下铝基陶瓷型芯的最佳脱脂温度为 500 °C,此时得到的陶瓷型芯样品 X 方向的收缩率为 2.3%, Y 方向的收缩率

为 1.9%, Z 方向的收缩率为 3.4%, 抗弯强度为 22.3 MPa, 开孔率为 35.6%。预埋粉末也会对陶瓷型芯的脱脂过程产生有利影响。Kong 等^[59]提出将增材制造的 Al₂O₃ 素坯在脱脂过程中埋入 SiO₂ 颗粒, 研究结果表明预埋 SiO₂ 粉末会增强 Al₂O₃ 颗粒之间的层间结合力, 减少样品的裂纹和局部变形。Yin 等^[60]进一步通过实验证明预埋硅粉会影响树脂挥发过程的化学平衡, 为陶瓷型芯的脱脂和烧结提供了支撑和稳定的热场, 此时样品内部的孔隙分布, 层间结合更加牢固。由于坯体周

围的高浓度和埋置粉末的毛细作用,样品内部树脂的分解将以均匀的速率发生^[61],使得掩埋样品的物理性质不易受加热速率的影响。

合适的烧结温度与升温速率有利于颗粒之间的结合,生成均匀的玻璃相,提升陶瓷型芯的性能。目前常采用的方法是通过对比在不同烧结温度和升温速率下烧结后的陶瓷型芯的各项物理性能,从而确定最佳的烧结工艺。Liu等^[62]认为当烧结温度由1200℃升至1250℃时,较高的烧结温度提供了更大的烧结驱动力,使得陶瓷型芯室温强度由7.5 MPa升至10.4 MPa,高温强度由6.5 MPa升至9.5 MPa。Dong等^[63]发现在1450℃烧结时大量热解产物分布在相邻的基体颗粒之间,形成烧结颈,陶瓷型芯具有28.394 MPa的室温强度与13.649 MPa的高温强度。Li等^[57]在升温阶段采用5℃/min的平缓加热速率将样品加热至不同的烧结温度 $T(T=1300、1350、1400、1450、1500、1550℃)$ 。随着烧结温度的升高,陶瓷型芯的孔隙率先增大后减小,在1400℃时达到最大值35%。抗折强度随烧结温度的升高而增大,但在1400℃时抗折强度的增量最大。在1300~1450℃下烧结的陶瓷型芯发生粒间开裂,在1500~1550℃下烧结时则发生穿晶破裂。这种断裂模式的差异主要归因于光固化增材制造工艺的逐层形成模式和烧结过程中各向异性收缩导致的层间结合力的差异。

真空浸渍作为一种孔隙调控技术,其原理是通过优化材料内部结构从而显著减少烧结过程中产生的缺陷。Park等^[64]将热处理后的型芯样品浸入无机前驱体中,然后干燥并在1000℃下热处理以进行有机-无机转化过程,经过此工艺处理后的素坯强度和烧结后的样品强度分别为 (18.1 ± 0.7) MPa和 (13.7 ± 0.8) MPa。Li等^[65]研究发现氧化铝溶胶的浸渍能促进硅基陶瓷型芯中方石英相的形成,而适量的方石英能提高陶瓷型芯的力学性能。Liu等^[66]通过真空浸渍技术加速了纳米SiO₂渗透至硅基陶瓷型芯这一过程,使得陶瓷型芯的密度增大,并促进了在1225℃烧结过程中方石英的形成,使得样品的高温强度达到23.55 MPa。Zhang等^[67]认为,在硅溶胶渗透过程中,大量的小二氧化硅颗粒会渗透至预烧结构。小的二氧化硅颗粒具有高表面能,促进了再烧结中液相的出现。液相的黏性流动有助于传质和颗粒的恢复,进而形成大的烧结颈。真空浸渍技术可以预填充孔隙,促进颗粒间的物质传输,减少烧结裂纹产生。

添加矿化剂可以促进或抑制基体材料的烧结,减少烧结缺陷。矿化剂的作用机理是与烧结过程中新生成的物相互相结合形成骨架从而提升陶瓷型芯的

性能^[68]。在陶瓷型芯中,适宜的方石英相含量可以起到高温强化与收缩缓冲作用。Gromada等^[69]在硅基陶瓷型芯中添加硼硅酸盐玻璃,其实验结果表明在烧结过程中石英玻璃的含量增加,材料的密度、抗弯强度提升的同时热膨胀系数降低。Liang等^[70]研究发现氧化铝的添加会促进烧结过程中熔融石英的结晶,增加方石英的含量。方石英和氧化铝的热膨胀系数均高于熔融石英,因此陶瓷型芯的热膨胀系数增加。Song等^[71]在硅基陶瓷型芯中添加不同含量的MgO,对比分析出MgO在不同烧结温度下的作用机制。在1200℃的初始烧结过程中,MgO促进了硅基陶瓷型芯中的非均质形核,加速了陶瓷型芯中方石英的结晶。此时MgO与熔融石英反应形成硅酸镁石,颗粒之间的结合增强,室温强度提高。在1550℃时,MgO与熔融SiO₂的反应促进了硅氧网络团簇之间的滑移,使得硅氧网络重排,阻碍了晶体生长,降低了玻璃态SiO₂的黏度,使生成的方石英含量先增大后减小。

莫来石具有高熔点与高硬度,生成莫来石相可以促进陶瓷型芯的烧结致密化。Liu等^[72]制备了不同粒径的二氧化硅与氧化铝的陶瓷浆料,较小的粒径增大了反应界面之间的有效接触面积,在烧结过程中促进了莫来石相的形成。Li等^[73]通过热力学计算进一步证实,方石英或熔融石英与 α -Al₂O₃之间的固-固反应是莫来石生成的主要路径,其吉布斯自由能负值在1100~1400℃区间最为显著,标志着在此温度区间更容易生成莫来石。Kim等^[74]将预烧结的多孔硅基样品浸泡在胶体氧化铝中,然后在1300℃下烧结。研究结果表明胶体氧化铝通过电荷相互作用附着在熔融石英表面,并在烧结过程中与熔融石英反应形成莫来石,从而抑制了熔融石英向方石英的结晶。这种莫来石化将硅基陶瓷型芯的抗弯强度从3.3 MPa提高到9.6 MPa,并将线收缩率从2%降低到1%。Yang等^[75]通过在光固化陶瓷浆料中添加氟化铝(AlF₃)和五氧化二钒(V₂O₅),利用气-固反应机制实现了莫来石晶须的原位生长。当氟化铝质量分数为9%时,晶须的形态和体积分数达到最优,使得陶瓷型芯室温强度提升69%,烧结收缩率下降73%。Qin等^[76]通过在熔融硅粉表面预涂覆氧化铝溶胶,形成高温稳定的刚玉/莫来石壳层,抑制液相烧结,从而维持陶瓷型芯的多孔均匀结构。An等^[77]使用了基于聚合物的聚乙烯亚胺(PEI)和基于硅烷的(3-氨基丙基)三乙氧基硅烷(APTES)作为前驱体,通过表面修饰纳米氧化铝粒子来引入氨基功能团。PEI接枝的氧化铝粒子渗透至基体中形成莫来石相,从而提高了陶瓷型芯的抗弯强

度。莫来石相能够有效连接打印层,提升层间结合力,具有良好的化学相容性和热稳定性。

除上述研究外,本文对部分矿化剂的影响及作用机制进行了总结,具体如表 3^[33,78-83]所示。

表 3 矿化剂对陶瓷型芯缺陷的影响

Table 3 Influence of sintering additives on ceramic core defects

Mineralizer	Research result	Mechanism analysis	Reference
Nano-SiO ₂	The contraction of the line first increases and then decreases; the flexural strength increases first and then decreases	The precipitation of glass phase, the combination of intergranular and intergranular mixed fracture modes, the pinning cracks of nanoparticles and the linkage of cracks lead to the reduction of fracture energy	[33]
SiB ₆	The linear shrinkage rate gradually decreases; the flexural strength at room temperature and high temperature only improves when the mass fraction of SiB ₆ is 0%-1.0%	The oxidation of SiB ₆ can inhibit the crystallization of fused quartz. The sintering promoting effect of B ₂ O ₃ generated by the reaction is at 1550 °C, the generated β-cristobalite has a relatively high strength, but the evaporation of B ₂ O ₃ weakens the improvement effect of β-cristobalite to a certain extent	[78]
ZrSiO ₄	Maintain high porosity; the room-temperature and high-temperature strength of the ceramic core has been enhanced	During the secondary sintering process, nano-ZrO ₂ reacts with large-particle SiO ₂ to form ZrSiO ₄ with a network structure. The formation of the ZrSiO ₄ network structure stabilizes the matrix and reduces the formation of defects	[79]
Metallic silicon powder	It inhibits the shrinkage rate; the curing thickness is reduced; the room-temperature strength and high-temperature strength are enhanced	Metal Si powder is transformed into SiO ₂ in the oxidation reaction and undergoes significant volume expansion, which inhibits the shrinkage rate. It partially fills the interlayer voids of the ceramic core and thickens the interlayer voids, reducing the occurrence of defects	[80]
Si ₃ N ₄	The relative density first increases and then decreases; the shrinkage rate decreases and the porosity increases; the strength at room temperature increases but slightly decreases at high temperatures	The increase in the content of Si ₃ N ₄ corresponds to the decrease in the content of amorphous SiO ₂ . Moreover, the surface of Si ₃ N ₄ particles has a SiO ₂ coating as an inert second phase, which inhibits the further crystallization of cristobalite. The oxidation of Si ₃ N ₄ will cause volume expansion, while the unoxidized Si ₃ N ₄ particles in the matrix will inhibit the densification process	[81]
Fe ₂ O ₃	The room-temperature strength and high-temperature strength of the core have both been improved	The addition of Fe ₂ O ₃ changes the ratio of bridged oxygen to non-bridged oxygen in the sample. Bridge oxygen restricts the nucleation of cristobalite during the high-temperature sintering process and inhibits the transformation of fused quartz to cristobalite. The relatively low content of cristobalite reduces the generation of microcracks	[82]
Photosensitive hydroxyl siloxane	The viscosity of the slurry has been reduced; the bulk density has been increased and the porosity has been reduced; the room-temperature strength and high-temperature strength increase	Form intermolecular hydrogen bonds with the hydroxyl groups on the surface of silica powder to prevent the agglomeration of silica powder; the sintering process transforms into an amorphous fused silica phase, which then crystallizes into a cristobalite phase. The small particles of cristobalite play a bonding role, promoting the formation of sintering necks among the large particles	[83]

纤维可以通过界面脱粘、裂纹偏转、纤维拔出等过程有效地耗散载荷能量,增加陶瓷型芯的强度。Niu 等^[84]研究发现莫来石纤维的添加显著降低了陶瓷型芯在烧结和铸造过程中的收缩率,并提高其抗蠕变性能。当莫来石纤维质量分数为 12.5% 时,陶瓷型芯

表现出最佳性能:孔隙率为 36.5%,高温抗弯强度为 21.2 MPa,三维方向的烧结收缩率分别为 0.87%、1.02% 和 1.13%,蠕变变形为 1.79 mm。莫来石纤维的表面可以与基体材料形成较强的界面结合,这种界面结合能够有效传递应力,减少应力集中现象,避免

缺陷的产生。莫来石纤维的无序分布和纤维拔出效应显著提高了陶瓷型芯的层间强度。Lu等^[85]在硅基陶瓷型芯中引入硅酸铝纤维(Al_2SiO_5)后,成功制备出具有优异性能的增强型硅基陶瓷型芯。由于异质形核和氧化铝扩散导致较低的晶化自由能, Al_2SiO_5 表面上存在非晶态 SiO_2 原位析出。随着纤维添加量的增加,方石英含量显著增加,同时在硅酸铝纤维表面发生了原位脱玻化现象,这有助于增强纤维与基体之间的界面结合强度。通过优化纤维和方石英晶种,样品表现出最低的烧结收缩率(0.38%)、最高的开孔率(47.1%)、近乎零的高温变形(0.07 mm)和12.86 MPa的高温抗弯强度。加入纤维能够形成均匀分布的孔隙,改善陶瓷型芯的孔隙结构,提高陶瓷型芯的热稳定性。

综上所述,现阶段调控脱脂-烧结缺陷的方法主要有优化脱脂-烧结工艺与添加矿化剂。通过综述脱脂-烧结气氛、脱脂-烧结时间、埋烧浸渍与不同种类矿化剂对陶瓷型芯缺陷的研究现状,发现改善脱脂-烧结工艺与添加矿化剂可以对陶瓷内部气体排出速率进行调控,使气体排出更为通畅,同时可以减少脱脂-烧结过程中的应力分布不均这一现象。将这两种措施相结合可以获得性能更为优异的陶瓷型芯。但目前尚未明确孔隙分布对陶瓷型芯微观组织的具体影响,仍需进一步研究。

3 结束语

高温合金空心涡轮叶片内部冷却流道越来越复杂,陶瓷型芯作为叶片内腔冷却流道成型的关键工艺部件,其性能直接影响叶片的精度和成品率。在光固化增材制造陶瓷型芯的过程中,打印缺陷与脱脂-烧结缺陷是影响陶瓷型芯成品率的主要原因。目前普遍认为打印缺陷包括打印孔隙、打印裂纹、打印错层、打印变形,这些打印缺陷会增大素坯的气孔率,降低素坯强度,影响打印精度;脱脂-烧结缺陷包括脱脂孔洞、脱脂裂纹、烧结孔洞和烧结裂纹,这些脱脂-烧结缺陷会降低陶瓷型芯的强度,影响陶瓷型芯的性能。通过改善浆料体系,优化打印参数可以控制打印缺陷,而采用合适的脱脂-烧结工艺,添加矿化剂则可以极大地改善脱脂-烧结缺陷。然而目前尚未探明固化机制与光传播过程中能量损耗之间的具体关联,孔隙分布对陶瓷型芯微观组织的影响也缺少深入研究,缺陷检测技术尚不完善。随着陶瓷型芯结构越来越复杂,未来增材制造陶瓷型芯制备技术将从以下三个重要方向发展:

(1)进一步探明固化行为与素坯缺陷的内在关系,深入理解固化过程中光敏树脂与陶瓷颗粒之间的相互作用,从而为优化打印工艺和浆料配方提供理论依据,最终减少打印缺陷,提高陶瓷型芯的质量。

(2)深入研究增材制造陶瓷型芯制备过程中孔隙分布演化规律对微观组织的影响,调控脱脂-烧结过程中气体逸出速率,最大程度地避免脱脂-烧结缺陷产生。

(3)将缺陷检测技术与人工智能技术相结合,建立增材制造陶瓷型芯缺陷数据库。以此为基础开发基于深度学习的缺陷检测技术,为增材制造陶瓷型芯缺陷预测和工艺优化提供新的技术手段。

参考文献

- [1] 刘国库,王威.航空发动机叶片制造及再制造技术研究[J].科技创新与应用,2022,12(33):145-148.
LIU G K, WANG W. Research on manufacturing and remanufacturing technology of aeroengine blades[J]. Technology Innovation and Application, 2022, 12(33): 145-148.
- [2] 陈荣章.航空铸造涡轮叶片合金和工艺发展的回顾与展望[J].航空制造技术,2002,45(2):19-23.
CHEN R Z. Review and prospect of developments of cast superalloys and technology of aeroengine turbine blade[J]. Aeronautical Manufacturing Technology, 2002, 45(2): 19-23.
- [3] 冯乐然.民用航空发动机涡轮叶片材料研究[J].中国设备工程,2022(7):268-269.
FENG L R. Study on turbine blade materials of civil aviation engine[J]. China Plant Engineering, 2022(7): 268-269.
- [4] PRADYUMNA R, BAIG M A H. Ceramic cores for turbine blades: a tooling perspective[J]. International Journal of Mechanical and Industrial Engineering, 2013: 93-99.
- [5] 刘小瀛,王宝生,张立同.氧化铝基陶瓷型芯研究进展[J].航空制造技术,2005,48(7):26-29.
LIU X Y, WANG B S, ZHANG L T. Research progress of alumina-based ceramic cores[J]. Aeronautical Manufacturing Technology, 2005, 48(7): 26-29.
- [6] 陈啸.涡轮叶片用氧化铝陶瓷型芯高温性能的研究[D].哈尔滨:哈尔滨工业大学,2009.
CHEN X. Study on the high temperature performance of alumina ceramic cores for investment casting turbine blades[D]. Harbin: Harbin Institute of Technology, 2009.
- [7] 翟小菲,陈婧祎,张学勤,等.陶瓷型芯3D打印研究进展与挑战[J].陶瓷学报,2023,44(5):831-848.
ZHAI X F, CHEN J Y, ZHANG X Q, et al. Recent progresses and challenges of 3D printing of ceramic cores[J]. Journal of Ceramics, 2023, 44(5): 831-848.
- [8] XU X Q, NIU S X, WANG X G, et al. Fabrication and casting simulation of composite ceramic cores with silica nanopowders[J]. Ceramics International, 2019, 45(15): 19283-19288.
- [9] 郝舒琪,苏海军,赵迪,等.粉体特性对光固化3D打印陶瓷浆料性质影响的研究进展[J].材料导报,2024,38(17):90-99.

- HAO S Q, SU H J, ZHAO D, et al. Research progress on the effect of powder characteristics on the properties of ceramic slurry based stereolithography 3D printing[J]. *Materials Reports*, 2024, 38(17): 90-99.
- [10] OZKAN B, SAMENI F, BIANCHI F, et al. 3D printing ceramic cores for investment casting of turbine blades, using LCD screen printers: the mixture design and characterisation[J]. *Journal of the European Ceramic Society*, 2022, 42(2): 658-671.
- [11] 胡可辉, 吕志刚, 陆宽, 等. 复杂陶瓷型芯增材制造及浇注工艺验证[J]. *机械工程学报*, 2021, 57(3): 227-234.
- HU K H, LÜ Z G, LU K, et al. Additive manufacturing of complex ceramic cores and verification of casting process[J]. *Journal of Mechanical Engineering*, 2021, 57(3): 227-234.
- [12] WANG F, LI Z J, LOU Y H, et al. Stereolithographic additive manufacturing of Luneburg lens using Al_2O_3 -based low sintering temperature ceramics for 5G MIMO antenna[J]. *Additive Manufacturing*, 2021, 47: 102244.
- [13] PUCHAKAYLA P K R, PEGU B, GANDHI P, et al. Defects evolution during printing, debinding and sintering for additive manufacturing of yttria stabilized zirconia[J]. *Materials Characterization*, 2025, 221: 114752.
- [14] LI H, LIU Y S, LI W B, et al. Effect of zirconia content and particle size on the properties of 3D-printed alumina-based ceramic cores[J]. *Journal of the American Ceramic Society*, 2021, 104(11): 6015-6028.
- [15] NIE G L, LI Y H, SHENG P F, et al. Microstructure refinement-homogenization and flexural strength improvement of Al_2O_3 ceramics fabricated by DLP-stereolithography integrated with chemical precipitation coating process[J]. *Journal of Advanced Ceramics*, 2021, 10(4): 790-808.
- [16] XING H Y, LAI L, ZHAO Y H, et al. Coating optimization of yield pseudoplastic paste-based stereolithography 3D printing of alumina ceramic core[J]. *Ceramics International*, 2022, 48(20): 30118-30126.
- [17] LI K W, JIANG W G, WANG S G, et al. Effect of specimen thickness on the creep deformation of a silica-based ceramic core material[J]. *Journal of Alloys and Compounds*, 2018, 763: 781-790.
- [18] LI X, SU H J, DONG D, et al. Selection strategy of curing depth for vat photopolymerization 3D printing of Al_2O_3 ceramics[J]. *Additive Manufacturing*, 2024, 88: 104240.
- [19] ZHENG W, WU J M, CHEN S, et al. Fabrication of high-performance silica-based ceramic cores through selective laser sintering combined with vacuum infiltration[J]. *Additive Manufacturing*, 2021, 48: 102396.
- [20] LI Q L, HOU W Q, LIANG J J, et al. Controlling the anisotropy behaviour of 3D printed ceramic cores: from intralayer particle distribution to interlayer pore evolution[J]. *Additive Manufacturing*, 2022, 58: 103055.
- [21] 陈静, 杨晓帅, 张鹏飞, 等. 光固化3D打印光敏树脂的临界能量和固化深度影响因素[J]. *科技导报*, 2024, 42(4): 110-114.
- CHEN J, YANG X S, ZHANG P F, et al. Studies on the influence factors on E_c and D_p of photocuring 3D printing photosensitive resin[J]. *Science & Technology Review*, 2024, 42(4): 110-114.
- [22] ZHAO D, SU H J, HU K H, et al. Formation mechanism and controlling strategy of lamellar structure in 3D printed alumina ceramics by digital light processing[J]. *Additive Manufacturing*, 2022, 52: 102650.
- [23] ZHANG T T, ZHAO S X, NIU X Y, et al. Preparation and properties of silica ceramic cores through direct writing technology[J]. *Ceramics International*, 2025, 51(19): 28186-28194.
- [24] YU X H, WANG Z G, LI Q L, et al. Spatial curing growth mechanism and defect control of alumina green bodies manufactured by stereo-lithography[J]. *Journal of the European Ceramic Society*, 2022, 42(6): 2931-2945.
- [25] CRAMER C L, WILT J K, CAMPBELL Q A, et al. Accuracy of stereolithography printed alumina with digital light processing[J]. *Open Ceramics*, 2021, 8: 100194.
- [26] LI H, LIU Y S, LIU Y S, et al. Effect of debinding temperature under an argon atmosphere on the microstructure and properties of 3D-printed alumina ceramics[J]. *Materials Characterization*, 2020, 168: 110548.
- [27] WANG K, QIU M B, JIAO C, et al. Study on defect-free debinding green body of ceramic formed by DLP technology[J]. *Ceramics International*, 2020, 46(2): 2438-2446.
- [28] SCHLACHER J, LUBE T, HARRER W, et al. Strength of additive manufactured alumina[J]. *Journal of the European Ceramic Society*, 2020, 40(14): 4737-4745.
- [29] QIU Y X, LI Q L, LIANG J J, et al. Control of sintering kinetics and thermal shock resistance for stereolithography 3D printed ceramics[J]. *Ceramics International*, 2025, 51(13): 17453-17462.
- [30] LI H, LIU Y S, LIU Y S, et al. Influence of vacuum debinding temperature on microstructure and mechanical properties of three-dimensional-printed alumina *via* stereolithography[J]. *3D Printing and Additive Manufacturing*, 2020, 7(1): 8-18.
- [31] LI H, LIU Y S, LIU Y S, et al. Microstructure and properties of 3D-printed alumina ceramics with different heating rates in vacuum debinding[J]. *Rare Metals*, 2020, 39(5): 577-588.
- [32] LI X, SU H J, DONG D, et al. New approach to preparing near zero shrinkage alumina ceramic cores with excellent properties by vat photopolymerization[J]. *Journal of Materials Science & Technology*, 2024, 193: 61-72.
- [33] LIU J Q, LI Q L, HUO M D, et al. Microstructure and mechanical properties of 3D-printed nano-silica reinforced alumina cores[J]. *Ceramics International*, 2022, 48(20): 30282-30293.
- [34] ZHANG L Z, LIU H, YAO H H, et al. 3D printing of hollow lattice structures of $\text{ZrO}_2(3\text{Y})/\text{Al}_2\text{O}_3$ ceramics by vat photopolymerization: process optimization, microstructure evolution and mechanical properties[J]. *Journal of Manufacturing Processes*, 2022, 83: 756-767.
- [35] ZHANG K Q, MENG Q Y, CAI N J, et al. Effects of solid loading on stereolithographic additive manufactured ZrO_2 ceramic: a quantitative defect study by X-ray computed tomography[J]. *Ceramics International*, 2021, 47(17): 24353-24359.
- [36] 谢昌平, 周彩楼, 陈涛, 等. 陶瓷注射成型混料工艺及坯体产生缺

- 陷研究[J].材料导报,2012,26(16):133-136,160.
- XIE C P, ZHOU C L, CHEN T, et al. Studies on mixing processes and defects of ceramic injection molding[J]. Materials Review, 2012, 26(16):133-136, 160.
- [37] 罗焯阳,杨现锋,刘子玉,等.3D打印陶瓷坯体热脱脂机理与工艺研究进展[J].硅酸盐通报,2024,43(10):3772-3786,3797.
- LUO H Y, YANG X F, LIU Z Y, et al. Research progress of mechanism and process of thermal debinding in 3D-printed ceramic green body[J]. Bulletin of the Chinese Ceramic Society, 2024, 43(10):3772-3786, 3797.
- [38] PAN Z P, GUO J Z, LI S M, et al. Experimental study on high temperature performances of silica-based ceramic core for single crystal turbine blades [J]. Ceramics International, 2022, 48(1): 548-555.
- [39] MITTS C, NABOULSI S, PRZYBYLA C, et al. Axisymmetric peridynamic analysis of crack deflection in a single strand ceramic matrix composite[J]. Engineering Fracture Mechanics, 2020, 235: 107074.
- [40] LI Q L, QIU Y X, HOU W Q, et al. Slurry flow characteristics control of 3D printed ceramic core layered structure: experiment and simulation [J]. Journal of Materials Science & Technology, 2023, 164:215-228.
- [41] TSENG W J, HSU C K. Cracking defect and porosity evolution during thermal debinding in ceramic injection moldings[J]. Ceramics International, 1999, 25(5):461-466.
- [42] SANTOLIQUIDO O, CAMEROTA F, ORTONA A. The influence of topology on DLP 3D printing, debinding and sintering of ceramic periodic architectures designed to replace bulky components[J]. Open Ceramics, 2021, 5:100059.
- [43] 李乔磊,顾玥,于雪华,等.烧结温度对3D打印硅基陶瓷型芯表面形貌及粗糙度的影响[J].无机材料学报,2022,37(3):325-332.
- LI Q L, GU Y, YU X H, et al. Effect of sintering temperature on surface morphology and roughness of 3D-printed silicon ceramic cores[J]. Journal of Inorganic Materials, 2022, 37(3):325-332.
- [44] GENTRY S P, HALLORAN J W. Depth and width of cured lines in photopolymerizable ceramic suspensions[J]. Journal of the European Ceramic Society, 2013, 33(10):1981-1988.
- [45] LI X Y, HU K H, LU Z G. Effect of light attenuation on polymerization of ceramic suspensions for stereolithography[J]. Journal of the European Ceramic Society, 2019, 39(7):2503-2509.
- [46] CAI P, GUO L, WANG H, et al. Effects of slurry mixing methods and solid loading on 3D printed silica glass parts based on DLP stereolithography[J]. Ceramics International, 2020, 46(10): 16833-16841.
- [47] AN X L, MU Y H, CHEN J W, et al. Compositional optimization of high-solid-loading ceramic cores *via* 3D printing [J]. Additive Manufacturing, 2022, 58:103054.
- [48] YANG Y K, WANG B R, LI J, et al. Solid loading optimization of ceramic slurry to achieve high-performance silica-based ceramic core through vat photopolymerization[J]. Ceramics International, 2024, 50(24):55307-55316.
- [49] GU Y, DUAN W Y, WANG T C, et al. Additive manufacturing of Al₂O₃ ceramic core with applicable microstructure and mechanical properties *via* digital light processing of high solid loading slurry[J]. Ceramics International, 2023, 49(15):25216-25224.
- [50] JIN F N, LI Q L, YANG K, et al. Optimisation and application of high solid loading stereolithography 3D printing ceramic cores slurry[J]. Ceramics International, 2024, 50(2):3574-3583.
- [51] CHEN X T, SUN J X, CAI P, et al. Enhancing precision in ceramic vat photopolymerization 3D printing through dispersant optimization[J]. Ceramics International, 2024, 50(22):45114-45124.
- [52] FAN J, LI Q L, JIN F N, et al. High solid loading, low viscosity stereolithography 3D printing ceramic cores slurry [J]. Ceramics International, 2023, 49(24):40705-40715.
- [53] KIM I, KIM S, ANDREU A, et al. Influence of dispersant concentration toward enhancing printing precision and surface quality of vat photopolymerization 3D printed ceramics [J]. Additive Manufacturing, 2022, 52:102659.
- [54] HU K H, WEI Y M, LU Z G, et al. Design of a shaping system for stereolithography with high solid loading ceramic suspensions [J]. 3D Printing and Additive Manufacturing, 2018, 5(4):311-318.
- [55] MU Y H, CHEN J W, AN X L, et al. Defect control in digital light processing of high-solid-loading ceramic core [J]. Ceramics International, 2022, 48(19):28739-28744.
- [56] OZKAN B, SAMENI F, GOULAS A, et al. Hot ceramic lithography of silica-based ceramic cores: the effect of process temperature on vat-photopolymerisation [J]. Additive Manufacturing, 2022, 58:103033.
- [57] LI Q L, AN X L, LIANG J J, et al. Balancing flexural strength and porosity in DLP-3D printing Al₂O₃ cores for hollow turbine blades[J]. Journal of Materials Science & Technology, 2022, 104: 19-32.
- [58] LI H, LIU Y S, LIU Y S, et al. Influence of debinding holding time on mechanical properties of 3D-printed alumina ceramic cores [J]. Ceramics International, 2021, 47(4):4884-4894.
- [59] KONG D K, GUO A F, HU Y B, et al. Alumina-based ceramic cores prepared by vat photopolymerization and buried combustion method[J]. Materials Today Communications, 2023, 37:107434.
- [60] YIN Y H, WANG J, HUANG Q Q, et al. Influence of debinding parameter and nano-ZrO₂ particles on the silica-based ceramic cores fabricated by stereolithography-based additive manufacturing [J]. Ceramics International, 2023, 49(12):20878-20889.
- [61] BAO Y, EVANS J R G. Kinetics of capillary extraction of organic vehicle from ceramic bodies. part I : flow in porous media [J]. Journal of the European Ceramic Society, 1991, 8(2):81-93.
- [62] LIU S Q, LI Q L, QU B Y, et al. Cooperative control of sintering shrinkage and strength of stereolithography 3D printed silica-based ceramic cores [J]. Ceramics International, 2025, 51(14): 19435-19448.
- [63] DONG W J, LI Q L, CHEN T C, et al. Effect of sintering temperature on microstructure and properties of 3D printing polysilazane reinforced Al₂O₃ core [J]. China Foundry, 2023, 20(5): 387-394.
- [64] PARK H Y, KIM E H, CHOI H H, et al. New conversion process for fabricating a ceramic core by a 3D printing technique [J]. Surface and Coatings Technology, 2017, 332:527-532.

- [65] LI H, HUANG Y Z, COLOMBO P. Effect of impregnation temperature and concentration of alumina sol on the properties of 3D printed silica ceramics [J]. *Materials Today Communications*, 2024, 41: 110616.
- [66] LIU H, ZHANG R Z, WU J M, et al. Effect of $\text{Al}(\text{OH})_3$ on the properties of silica-based ceramic cores prepared by laser powder bed fusion combined with vacuum infiltration [J]. *Additive Manufacturing*, 2024, 95: 104527.
- [67] ZHANG J, WU J M, LIU H, et al. Microstructure and properties of silica-based ceramic cores by laser powder bed fusion combined with vacuum infiltration [J]. *Journal of Materials Science & Technology*, 2023, 157: 71-79.
- [68] 陈天赐, 李乔磊, 张辉, 等. 矿化剂对陶瓷型芯性能的影响 [J]. *铸造*, 2022, 71(10): 1262-1270.
- CHEN T C, LI Q L, ZHANG H, et al. Effect of mineralizers on properties of ceramic core [J]. *Foundry*, 2022, 71(10): 1262-1270.
- [69] GROMADA M, ŚWIECA A, CYGAN R. The effect of additives on properties of silica-based ceramic cores utilised in fabrication of multivane clusters for turbofan jet engine [J]. *Ceramics International*, 2022, 48(17): 25621-25627.
- [70] LIANG J J, LIN Q H, ZHANG X, et al. Effects of alumina on cristobalite crystallization and properties of silica-based ceramic cores [J]. *Journal of Materials Science & Technology*, 2017, 33(2): 204-209.
- [71] SONG H R, XUAN W D, ZHOU X, et al. Effect of MgO on phase transformation and microstructural properties of silica-based ceramic cores [J]. *Ceramics International*, 2025, 51(18): 25520-25530.
- [72] LIU F, XU Q Z, QU J J, et al. Effect of silica particle size on the viscosity, curing behavior, and sintering performance of silica/alumina ceramic suspensions for digital light processing-based vat photopolymerization [J]. *Ceramics International*, 2025, 51(17): 23459-23470.
- [73] LI Q L, MENG X T, ZHANG X C, et al. Enhanced 3D printed Al_2O_3 core *via in-situ* mullite [J]. *Additive Manufacturing*, 2022, 55: 102826.
- [74] KIM Y H, YEO J G, CHOI S C. Shrinkage and flexural strength improvement of silica-based composites for ceramic cores by colloidal alumina infiltration [J]. *Ceramics International*, 2016, 42(7): 8878-8883.
- [75] YANG Y K, WANG A R, ZHOU Y L, et al. *In-situ* grown mullite whiskers zipper the printing layers in silica-based ceramic cores through vat photopolymerization 3D printing [J]. *Ceramics International*, 2025, 51(10): 12622-12633.
- [76] QIN Y, SUN X S, CHENG Y N, et al. Boosting the collapse performance of wax-binder-free silica based ceramic core *via* adding nano-alumina sol modified fused silica powder [J]. *Journal of Sol-Gel Science and Technology*, 2024, 111(3): 659-670.
- [77] AN G S, CHOI S W, KIM T G, et al. Amino-functionalization of colloidal alumina particles for enhancement of the infiltration behavior in a silica-based ceramic core [J]. *Ceramics International*, 2017, 43(1): 157-161.
- [78] ZHENG W, WU J M, CHEN S, et al. Improved mechanical properties of SiB6 reinforced silica-based ceramic cores fabricated by 3D stereolithography printing [J]. *Ceramics International*, 2022, 48(15): 21110-21117.
- [79] LI Q L, LIANG J J, ZHANG Y L, et al. Fused silica ceramic core based on network-structured zircon design *via* 3D printing [J]. *Scripta Materialia*, 2022, 208: 114342.
- [80] LI J, NIU S X, LI X, et al. Inter-layer structures regulated by metallic Si powders in 3D printing of silica-based ceramic cores [J]. *Ceramics International*, 2024, 50(13): 23389-23399.
- [81] XUAN W D, ZHANG Q, SONG H R, et al. Improved mechanical properties and dimensional accuracy of silica-based ceramic cores by Si_3N_4 addition [J]. *Ceramics International*, 2024, 50(14): 25730-25737.
- [82] QU B Y, LI Q L, LIU S Q, et al. Controlling the cristobalite content, microstructure, and properties of vat photopolymerization 3D printed SiO_2 -based ceramic cores by doping Fe_2O_3 [J]. *Ceramics International*, 2025, 51(12): 15535-15546.
- [83] ZHANG K L, DONG X, CHEN Y, et al. Influence of photosensitive hydroxy siloxane on the mechanical properties of silicon-based ceramic cores prepared by digital light processing [J]. *Ceramics International*, 2025, 51(3): 3394-3403.
- [84] NIU S X, WANG K, LUO Y S, et al. Enhanced high-temperature dimensional accuracy by fibers in silica ceramic cores prepared through vat photopolymerization 3D printing [J]. *Ceramics International*, 2024, 50(14): 25886-25894.
- [85] LU G, WU Q, CHEN X, et al. *In-situ* surface devitrification and properties enhancement of silica-based ceramic cores reinforced with aluminosilicate fibers and pre-added cristobalite seeds [J]. *Ceramics International*, 2025, 51(7): 8709-8718.

基金项目:国家自然科学基金(52402094, U234120139, U22A20129); 辽宁省科学技术计划项目(2024JH2/101900011); 国家重点研发计划(2024YFB3714504, 2024YFB3714503); 国防基础科研计划(JCKY2022130C005); 中国博士后科学基金(2023M743571); 国家资助博士后研究人员计划(GZC20232743); 中国科学院金属研究所创新基金(2024-PY11); 高端装备铸造技术全国重点实验室开放基金(CAT2023-006); 安徽省研究生教育质量工程(2023cxcysj015)

收稿日期:2025-06-30; **录用日期:**2025-08-03

通讯作者:李乔磊(1993—), 男, 助理研究员, 博士, 研究方向为增材制造陶瓷材料及单晶高温合金叶片精密铸造, 联系地址: 辽宁省沈阳市沈河区文化路72号(110016), E-mail: qlli@imr.ac.cn

(本文责编: 齐书涵)